

# Conformal Mesh Mappings

Bachelor Thesis D-MATH ETHZ  
Alessandra Iacopino  
Supervisor: Prof. Dr. Ralf Hiptmair

## Abstract

Given a 2D triangular mesh  $\widehat{\mathcal{M}}$  of the unit disk  $\mathbb{D}$ , whose triangles are all nicely shape-regular (in the sense that the ratio of their diameter to the radius of the largest inscribed circle is uniformly bounded for all triangles), we are guaranteed the existence of a conformal mapping  $\Phi$  from  $\mathbb{D}$  to any simply connected bounded domain  $\Omega$  by the Riemann mapping theorem. This allows for a sufficiently "nice" mesh  $\mathcal{M}$  on  $\Omega$  to be obtained as the image of  $\widehat{\mathcal{M}}$  under  $\Phi$ , i.e.  $\mathcal{M} = \Phi(\widehat{\mathcal{M}})$ . The challenge lies in the numerical construction/ approximation of this conformal mapping  $\Phi$ . This text is intended to give a general overview of currently known numerical conformal mapping algorithms, and to provide a comparison in terms of accuracy, runtime, and the representation format of the resulting map, particularly emphasizing the efficiency of point evaluations for both the mapping  $\Phi$  itself and its derivative (Jacobian)  $D\Phi$ . Finally, we implement [Algorithm Name](#).

# Contents

<b>1</b>	<b>Introduction</b>	<b>4</b>
<b>2</b>	<b>Theoretical Background</b>	<b>5</b>
2.1	Conformal Mappings . . . . .	5
2.2	Riemann Mapping Theorem . . . . .	5
2.2.1	Preliminary Results . . . . .	6
2.2.2	Proof of Riemann Mapping Theorem . . . . .	8
2.3	Reformulation as Boundary Value Problem . . . . .	10
2.4	Boundary Conditions . . . . .	11
2.4.1	Dirichlet Boundary Conditions . . . . .	11
2.4.2	Neumann Boundary Conditions . . . . .	11
2.5	Solution of the Boundary Value Problem via Fredholm Integral Equations of the Second Kind . . . . .	12
2.5.1	Neumann Kernel . . . . .	12
2.5.2	Hilbert Transform . . . . .	12
2.6	Sobolev Spaces . . . . .	12
2.7	Riemann-Hilbert Problems . . . . .	13
2.8	Complex Analysis/ Function Theoretic Tools . . . . .	13
2.9	Meshes . . . . .	14
2.10	Mesh Structure . . . . .	14
2.11	Crowding . . . . .	14
2.11.1	The operator $R$ . . . . .	14
<b>3</b>	<b>Existing Methods</b>	<b>16</b>
3.1	Bergman Kernel Method . . . . .	16
3.2	Preprocessing . . . . .	16
3.2.1	Osculation Methods . . . . .	16
3.3	Alternating Projections Method . . . . .	16
3.3.1	Alternating Projections à la von Neumann . . . . .	17
3.3.2	Algorithm . . . . .	17
3.4	Schwarz-Christoffel Method . . . . .	17
3.4.1	Preliminaries and Notation . . . . .	17
3.4.2	the log derivative of $\Phi$ . . . . .	18
3.4.3	Green's Functions . . . . .	18
3.4.4	Schwarz-Christoffel Equation Variants . . . . .	18
3.4.5	Implementation . . . . .	19
3.5	Zipper Method . . . . .	19
3.5.1	The Geodesic Algorithm . . . . .	19
3.5.2	The Slit Algorithm . . . . .	20
3.5.3	The Zipper Algorithm . . . . .	20
3.6	Newton/ Wegmann Method . . . . .	21
3.6.1	Implementation . . . . .	21
3.7	Theodorsen's Method . . . . .	22
3.8	Conjugate Function Method . . . . .	23

3.9	Amano's Method of Fundamental Solutions . . . . .	23
3.10	Probabilistic Uniformization Method . . . . .	23
3.11	Comparison . . . . .	23
<b>4</b>	<b>Proposed Method</b>	<b>26</b>
4.1	Choice/ Justification . . . . .	26
4.2	Implementation . . . . .	26
4.3	Numerical Experiments/ Testing . . . . .	26
4.4	Results . . . . .	26
<b>5</b>	<b>Conclusion</b>	<b>27</b>
<b>6</b>	<b>Documentation and Implementation</b>	<b>28</b>
6.1	Testing (again?) . . . . .	28
	<b>Bibliography</b>	<b>29</b>

## 1 Introduction

Given a 2D triangular mesh  $\widehat{\mathcal{M}}$  of the unit disk  $\mathbb{D}$ , whose triangles are all nicely shape-regular (in the sense that the ratio of their diameter to the radius of the largest inscribed circle is uniformly bounded for all triangles), we are guaranteed the existence of a conformal mapping  $\Phi$  from  $\mathbb{D}$  to any simply connected bounded domain  $\Omega$  by the Riemann mapping theorem. This allows for a sufficiently "nice" mesh  $\mathcal{M}$  on  $\Omega$  to be obtained as the image of  $\widehat{\mathcal{M}}$  under  $\Phi$ , i.e.  $\mathcal{M} = \Phi(\widehat{\mathcal{M}})$ .

In this article we study the problem of numerically constructing conformal mappings, given a mesh on the disk and the target domain by its boundary. We first review the theoretical background of conformal mappings and present a proof of the famous Riemann Mapping Theorem. We then review several existing numerical methods for approximating such mappings. The methods are compared in terms of accuracy of the approximation, computational complexity and efficiency of point evaluations for both the mapping  $\Phi$  itself and its derivative (Jacobian)  $D\Phi$ .

Finally, **Algorithm Name** is implemented in Python. The algorithm is tested on several target domains and the results are discussed.

## 2 Theoretical Background

THROUGHOUT THIS PAPER, WE ASSUME TO BE GIVEN A SIMPLE CONNECTED REGION  $\Omega \subset \mathbb{C}$  GIVEN BY ITS BOUNDARY  $\partial\Omega$  WHICH IS PARAMETRIZED BY A DIFFERENTIABLE  $2\pi$ -PERIODIC COMPLEX FUNCTION  $\eta(s)$  WITH CONTINUOUS NON-VANISHING DERIVATIVE.

### 2.1 Conformal Mappings

#### Definition 1

A **conformal mapping**, also called a conformal map, conformal transformation, angle-preserving transformation, or biholomorphic map, is a transformation  $f(z)$  that preserves local angles. An analytic function is conformal at any point where it has a nonzero derivative.

#### Definition 2

A **complex analytic function** or **holomorphic function** on an open subset  $U \subset \mathbb{C}$  is locally given by a convergent power series, i.e. for any  $x_0 \in U$  there exists a neighborhood  $V \subset U$  of  $x_0$  such that for all  $z \in V$  we have

$$f(z) = \sum_{n=0}^{\infty} a_n(z - z_0)^n$$

for some complex coefficients  $a_n \in \mathbb{C}$ . The terms analytic and holomorphic are used interchangeably.

### 2.2 Riemann Mapping Theorem

#### Definition 3

We call a subset  $\Omega \subset \mathbb{C}$  **proper** if  $\emptyset \neq \Omega \neq \mathbb{C}$ .

#### Theorem 2.1 (Riemann Mapping Theorem)

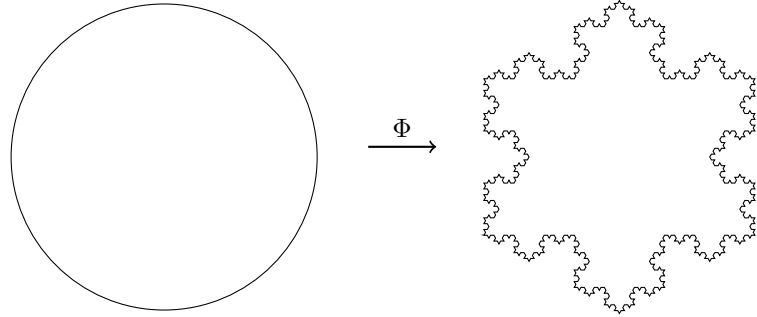
If  $\Omega$  is a non-empty simply connected open proper subset of the complex plane  $\mathbb{C}$ , then there exists a biholomorphic mapping  $f$  (i.e. a bijective holomorphic mapping whose inverse is also holomorphic) from  $\Omega$  onto the open unit disk

$$D = \{z \in \mathbb{C} : |z| < 1\}.$$

This mapping is known as a Riemann mapping.

The beauty of the Riemann mapping theorem lies in its weight of implications, i.e. the fact that it guarantees the existence of a conformal map between any two simply connected domains in the complex plane, provided they are not the entire plane. The existence of this Riemann map is a priori not obvious: Even relatively simple Riemann mappings (for example a map from the interior of a circle to the interior of a square) have no explicit formula using only elementary functions. Simply connected open sets in the plane can be highly complicated, for instance, the boundary can be a nowhere-differentiable fractal

curve of infinite length, even if the set itself is bounded. One such example is the Koch curve. The fact that such a set can be mapped in an angle-preserving manner from the nice and regular unit disc seems counter-intuitive.



We closely follow the proof by normal families in [SS03].

### 2.2.1 Preliminary Results

**Lemma 2.2** (Schwarz Lemma)

Let  $f : \mathbb{D} \rightarrow \mathbb{D}$  be holomorphic with  $f(0) = 0$ . Then

1.  $|f(z)| \leq |z|$  for all  $z \in \mathbb{D}$ .
2. If for some  $z_0 \neq 0$  we have  $f(z_0) = z_0$  then  $f$  is a rotation.
3.  $|f'(0)| \leq 1$  and if equality holds, then  $f$  is a rotation.

*Proof.* See [SS03] page 218.

### Definition 4

A family  $\mathcal{F}$  of holomorphic functions on a domain  $\Omega$  is called **normal** if every sequence in  $\mathcal{F}$  contains a subsequence that converges uniformly on any compact subset of  $\Omega$ .

### Definition 5

A family  $\mathcal{F}$  is called **uniformly bounded on compact subsets** of  $\Omega$  if for every compact subset  $K \subset \Omega$  there exists a constant  $M_K$  such that  $|f(z)| \leq M_K$  for all  $z \in K$  and all  $f \in \mathcal{F}$ .

### Definition 6

A family  $\mathcal{F}$  of holomorphic functions on a domain  $\Omega$  is called **equicontinuous** if for every  $\epsilon > 0$  there exists a  $\delta > 0$  such that if  $z \in \Omega$  with  $|z - z_0| < \delta$  we have  $|f(z) - f(z_0)| < \epsilon$  for all  $f \in \mathcal{F}$ .

### Theorem 2.3 (Montel)

A family  $\mathcal{F}$  of holomorphic functions on  $\Omega$  that is uniformly bounded on compact subsets of  $\Omega$  is normal if and only if it is equicontinuous on compacta.

*Proof.* See [SS03] page 225.

**Theorem 2.4** (Hurwicz)

Let  $\Omega \subset \mathbb{C}$  be a connected open subset and let  $f_n : \Omega \rightarrow \mathbb{C}$  be a sequence of injective holomorphic functions that converges uniformly on compact subsets of  $\Omega$  to a holomorphic function  $f \neq 0$ . If  $f$  has a zero of order  $m$  at  $z_0$  then for every  $\varepsilon > 0$  and sufficiently large  $k = k(\varepsilon) \in \mathbb{N}$   $f_k$  has precisely  $m$  zeros in  $B_\varepsilon(z_0)$  including multiplicities. Moreover, the zeros converge to  $z_0$  as  $k \rightarrow \infty$ .

We will use the following corollary of Hurwicz' theorem in the proof of 2.1:

**Corollary 2.5** (Uniform Convergence to Holomorphic Limit and Injectivity)

Let  $\Omega \subset \mathbb{C}$  be a connected open subset and let  $f_n : \Omega \rightarrow \mathbb{C}$  be a sequence of injective holomorphic functions that converges uniformly on compact subsets of  $\Omega$  to a holomorphic function  $f$ . Then  $f$  is either constant or injective.

*Proof.?*

**Proposition 2.6** (Cauchy Inequality)

Let  $f$  be holomorphic on an open set containing the closure of a ball  $B_R(z_0)$  centered at  $z_0$  of radius  $R$ . Then

$$|f^{(n)}(z_0)| \leq \frac{n! \|f\|_C}{R^n},$$

where  $\|f\|_C = \sup_{z \in C} |f(z)|$  on the boundary circle  $C$ .

*Proof.* See [SS03] page 48.

**Theorem 2.7** (Maximum Modulus Principle)

Let  $\Omega \subset \mathbb{C}$  be a connected open bounded set and  $f : \Omega \rightarrow \mathbb{C}$  holomorphic. If  $z_0$  is a point in  $\Omega$  such that  $|f(z_0)| \geq |f(z)|$  for all  $z$  in a neighborhood of  $z_0$ , then  $f$  is constant on  $\Omega$ .

*Proof.* See [SS03] page 92.

**Theorem 2.8** (Implicit Mapping Theorem)

Let  $r > 0$  be a radius, and let  $x_0 \in \mathbb{R}^n$ ,  $y_0 \in \mathbb{R}^m$ . Consider the open set  $W = B_r(x_0) \times B_r(y_0) \subset \mathbb{R}^n \times \mathbb{R}^m$  defined as

$$W = \{(x, y) \in \mathbb{R}^n \times \mathbb{R}^m : \|x - x_0\|_2 < r \text{ and } \|y - y_0\|_2 < r\}.$$

Let  $F : W \rightarrow \mathbb{R}^m$  be a continuous function satisfying the following conditions:

1.  $F(x_0, y_0) = 0$ .
2. The partial derivatives  $\partial_{y_k} F : W \rightarrow \mathbb{R}^m$  exist for all  $k \in \{1, \dots, m\}$  and are continuous on  $W$ .
3. The partial differential  $D_y F(x_0, y_0)$  (the differential of the map  $y \mapsto F(x_0, y)$  at  $y_0$ ) is invertible.

Then there exist radii  $\alpha, \beta \in (0, r)$  such that for the open balls  $U_0 = B_\alpha(x_0) \subset \mathbb{R}^n$  and  $V_0 = B_\beta(y_0) \subset \mathbb{R}^m$ , there exists a unique continuous function  $f : U_0 \rightarrow V_0$  satisfying:

- $f(x_0) = y_0$ .
- $\forall (x, y) \in U_0 \times V_0 : F(x, y) = 0 \iff y = f(x)$ .

*Proof.* See [EW22] page 573.

### 2.2.2 Proof of Riemann Mapping Theorem

*Step 1: Existence of a bounded injective holomorphic map to the unit disk*

Let  $\Omega$  be a simply connected open proper subset of  $\mathbb{C}$ . We show that  $\Omega$  is conformally equivalent to an open subset of the unit disk containing the origin. Indeed, choose  $\alpha \notin \Omega$  and consider the function

$$f(z) := \log(z - \alpha)$$

on  $\Omega$ , which is well-defined and holomorphic since  $z - \alpha$  never vanishes on  $\Omega$ . Note  $f$  is injective since  $e^{f(z)} = z - \alpha$  is  $(f(z_1) = f(z_2) \implies z_1 - \alpha = z_2 - \alpha)$ . Then for a point  $\omega \in \Omega$  we get  $f(z) \neq f(\omega) + 2\pi i \quad \forall z \in \Omega$  since otherwise we would find  $z = \omega$  again by exponentiating. In fact,  $f(z) \cap B_\epsilon(f(\omega) + 2\pi i) = \emptyset$  for some  $\epsilon > 0$  since otherwise we would find a sequence  $z_n \rightarrow \omega$  with  $f(z_n) \rightarrow f(\omega) + 2\pi i$ , contradicting the continuity of  $f$ . Finally, the function

$$g(z) := \frac{1}{f(z) - (f(\omega) + 2\pi i)}$$

is well-defined, holomorphic and injective on  $\Omega$  and maps  $\Omega$  to a bounded subset  $g(\Omega) \subset \mathbb{C}$ , so  $g$  is conformal. By boundedness of  $g(z) < \frac{1}{\epsilon}$  we can scale and translate  $g(\Omega)$  to contain the origin and fit into the unit disk.

*Step 2: Normalization and non-zero derivative*

By step 1 we can assume  $\Omega$  to be an open subset of the unit disk with  $0 \in \Omega$ . Consider the family

$$\mathcal{F} := \{f : \Omega \hookrightarrow \mathbb{D} | f(0) = 0\}$$

of all injective holomorphic functions which map the origin to itself. Note that  $\mathcal{F} \neq \emptyset$  since it contains the identity, and it is a uniformly bounded family by construction (maps into unit disk). In order to use the Hurwitz corollary and get injectivity, we now want to find a function  $f \in \mathcal{F}$  that maximizes  $|f'(0)|$  (to rule out constant functions yielded otherwise by the application of said corollary). Observe that by the Cauchy inequality 2.6  $|f'(0)|$  are uniformly bounded for  $f$  in  $\mathcal{F}$ . Next, let

$$s := \sup_{f \in \mathcal{F}} |f'(0)|.$$

and choose a sequence  $f_n \subset \mathcal{F}$  such that  $|f'_n(0)| \rightarrow s$  as  $n \rightarrow \infty$ . By Montel's theorem,  $f_n$  has a subsequence converging uniformly on compacta to a holomorphic  $f$  on  $\Omega$ . Since  $s \geq 1$  (the identity is in  $\mathcal{F}$ ),  $f$  is non-constant. Hence by the

Hurwicz corollary 2.5,  $f$  must be injective. By continuity we have  $|f(z)| \leq 1$  for all  $z \in \Omega$ , and since  $f$  is non-constant, by the Maximum Modulus Principle 2.7  $|f(z)| < 1$ . Finally and since  $f(0) = 0$ , we have  $f \in \mathcal{F}$  and  $|f'(0)| = s$ .

*Step 3: Conformal mapping to the entire disk*

By injectivity it suffices to show  $f$  is surjective. Suppose towards a contradiction that  $f$  is not surjective, we will construct a function in  $\mathcal{F}$  with derivative greater than  $s$  at the origin. So let  $\alpha \in \mathbb{D}$  be such that  $\alpha \notin f(\Omega)$  and consider the automorphism of the unit disk that interchanges 0 and  $\alpha$ ,

$$\psi_\alpha(z) := \frac{\alpha - z}{1 - \bar{\alpha}z}.$$

Since  $\Omega$  is simply connected and by continuity of  $f$  and  $\psi_\alpha(\Omega)$ , the set  $U := (\psi_\alpha \circ f)(\Omega)$  is simply connected and does not contain the origin. Thus we can define a square root function on  $U$  by

$$q(w) = e^{\frac{1}{2}\log w}.$$

Next, consider the function

$$F = \psi_{q(\alpha)} \circ q \circ \psi_\alpha \circ f.$$

Then  $F \in \mathcal{F}$  since  $F(0) = 0$  and  $F$  is holomorphic and injective since all the composing functions are. Also,  $F$  maps into the unit disk since all the composing functions do. But now if  $h$  denotes the square function  $h(w) = w^2$ , then we must have

$$f = \psi_\alpha^{-1} \circ h \circ \psi_{q(\alpha)}^{-1} \circ F = \Phi \circ F.$$

But  $\Phi : \mathbb{D} \rightarrow \mathbb{D}$  satisfies  $\Phi(0) = 0$  and is not injective since  $F$  is but  $h$  is not. By the Schwarz lemma 2.2 we get  $|\Phi'(0)| < 1$  and hence

$$|f'(0)| = |\Phi'(0)||F'(0)| < |F'(0)|,$$

contradicting maximality of  $|f'(0)|$  in  $\mathcal{F}$ .

Finally, multiplying  $f$  with a suitable unimodular complex number gives the desired conformal map from  $\Omega$  to  $\mathbb{D}$  with

$$\psi(0) = 0, \quad \psi'(0) > 0. \tag{1}$$

**REPLACE F BY PSI EVERYWHERE** □

### Corollary 2.9

Any two simple connected open proper subsets of  $\mathbb{C}$  are conformally equivalent.

*Proof.* This follows directly from the Riemann mapping theorem by taking the unit disk as an intermediate step. □

### Theorem 2.10 (Carathéodory)

The conformal mapping  $\Phi : \mathbb{D} \rightarrow \Omega$  can be extended to a continuous mapping  $\Phi : \bar{\mathbb{D}} \rightarrow \bar{\Omega}$  if the boundary  $\Gamma = \partial\Omega$  consists of a closed curve. [Weg05], p. 357

*Proof.* See [Pom92] page 24.

Existence established, the problem now becomes the explicit construction of a conformal mapping. Once the boundaries of the domain and target region are conformally mapped, the interior can be deduced from the boundary by the Cauchy Integral Formula. Hence why the main focus of the task lies on mapping boundary to boundary.

The strategy for numerical construction of the boundary mapping is to transform it into a boundary value problem.

### 2.3 Reformulation as Boundary Value Problem

When the region  $\Omega$  is bounded by a closed Jordan curve  $\Gamma$  the mapping  $\psi : \mathbb{D} \rightarrow \Omega$  can be extended continuously to the closure  $\bar{\mathbb{D}}$  by Carathéodory's Extension Theorem 2.10. Then the boundary can be parametrized by a  $2\pi$ -periodic function  $\eta$  in counterclockwise direction (positive orientation, aka *normal representation* [Weg05], page 387) and the mapping  $\psi$  is determined by its boundary values

$$\psi(e^{it}) = \eta(S(t)) \quad (2)$$

for  $t \in [0, 2\pi]$  and  $S$  the **boundary correspondence function**. By the implicit mapping theorem 2.8, the conformal mapping  $\psi$  depends on the boundary curve of  $\Omega$  by the boundary correspondence equation 2.

a rh problem arises when considering the change of the conformal mapping under changes to the boundary curve. weg388

From Definition 1 we know that a complex differentiable function with non-vanishing complex derivative is conformal, and complex differentiability in two dimensions can be characterised by the Cauchy-Riemann equations (necessary and sufficient condition). Denoting

$$J := \begin{pmatrix} \partial_x & -\partial_y \\ \partial_y & \partial_x \end{pmatrix}$$

we want to find a deformation  $\psi = u + iv$  such that  $J\psi = 0$ .

As a byproduct of the Cauchy-Riemann equations, both components of a conformal map are harmonic functions, i.e. they satisfy Laplace's equation  $\Delta u = 0 = \Delta v$  PROOF. Thus, one way to construct conformal maps is to solve Laplace's equation with suitable boundary conditions.

#### Definition 7

Two harmonic functions  $u(x, y)$  and  $v(x, y)$  on a domain are called **conjugate** if they satisfy the Cauchy-Riemann equations on the domain. E.g.  $v$  is a conjugate for  $u$ , and  $-u$  is a conjugate for  $v$ .

This directly leads to the conclusion that it suffices to find only one of the components of  $\psi = u + iv$ , since the other one can then be deduced as its conjugate harmonic function. This formulation is called the **Dirichlet problem** for

the Laplace equation. It can be described as finding  $\psi$  analytic in  $\mathbb{D}$ , continuous in  $\overline{\mathbb{D}}$  and satisfying

$$\begin{aligned} \operatorname{Re}(\psi(e^{it})) &= \eta(S(t)) && \text{on } \partial\mathbb{D} \\ \Delta u &= 0 && \text{in } \mathbb{D}^\circ, \end{aligned} \quad (3)$$

where  $\psi$  is  $2\pi$ -periodic and Hölder continuous. This problem has a unique solution up to an imaginary constant, which can be constructed using the conjugation operator

$$K\psi(s) := \frac{1}{2\pi} \int_0^{2\pi} \psi(t) \cot\left(\frac{s-t}{2}\right) dt,$$

which is also known as Hilbert Transform (details on this in [CR25]). In principle, we have two options for finding conformal mappings, namely to solve linear or non-linear boundary value problems. The linear problems are naturally faster to solve numerically, however their kernels must be adapted to each new fixed boundary and thus these methods present complications when dealing with pre-defined boundaries. Non-linear methods on the other hand can be more flexible with respect to the boundary shape, but are computationally more expensive.

## 2.4 Boundary Conditions

### Remark 1

Note that the Cauchy-Riemann equations do not guarantee a solution for arbitrary boundary data. A holomorphic map from the boundary of the unit disk onto some boundary of a convex set in  $\mathbb{C}$  satisfies Cauchy-Riemann equations if the boundary of the target set can be described by non-negative Fourier frequencies [PROOF]. Thus, the choice of parametrization of the target region's boundary is usually another challenge posed when solving conformal mapping problems, but for the scope of this article we assume to be given a suitable parametrization of  $\partial\Omega$ .

#### 2.4.1 Dirichlet Boundary Conditions

#### 2.4.2 Neumann Boundary Conditions

In order to use numerical methods efficiently via the [Fast Fourier Transform def?](#) we will prefer the functions' Fourier series representations. Hence on a grid of  $N = 2n$  equidistant [why? FFT requires it? has crowding as an effect...](#) points  $t_j = \frac{(j-1)2\pi}{N}$ ,  $\psi$  will be written as

$$\psi(t_j) = \sum_{k=-n+1}^n c_k e^{ikt_j} \text{ for } j \in [N]$$

and the conjugation operator can be approximated by the operator  $K_N$  defined as

$$K_N \psi(t_j) = \sum_{k=1}^{n-1} -ic_k e^{ikt_j} + ic_{-k} e^{-ilt_j}.$$

The function  $K_N$  is thus defined as a trigonometric polynomial obtained by interpolating  $\psi$  at the grid points. This approximation of the actual operator  $K$  satisfies

$$\|K\psi - K_N\psi\|_\infty \in O(n^{-\alpha+1/2})$$

for  $\psi \in C^\alpha$  Hölder continuous. If  $\psi$  is smoother, e.g.  $\psi \in C^{k-1}$ , the error decreases to

$$\|K\psi - K_N\psi\|_\infty \in O(n^{-k} \log(n) \|\psi^{(k)}\|_{inf_{t,y}})$$

[Weg05] p. 362. add more details on this operator?

## 2.5 Solution of the Boundary Value Problem via Fredholm Integral Equations of the Second Kind

We often numerically solve BVPs by transforming them into integral equations. Integral equations are equations in which an unknown function appears under an integral sign. They are classified into two main types: Fredholm and Volterra integral equations. Fredholm integral equations have fixed limits of integration, while Volterra integral equations have variable limits of integration. Both types can be further categorized into first kind and second kind, depending on whether the unknown function appears only under the integral sign or also outside of it.

### Definition 8

A Fredholm integral equation of the second kind is an equation of the form

$$f(x) = \lambda \int_a^b K(x, t)\phi(t)dt + g(x)$$

where  $f$  and  $g$  are known functions,  $\phi$  is the unknown function to be solved for,  $K(x, t)$  is a given kernel function, and  $\lambda$  is a constant.

There are several methods to solve Fredholm integral equations of the second kind, which we will explore in what follows...

### 2.5.1 Neumann Kernel

NEUMANN KERNEL?[Gai64] used to solve fredholm integral eq of the second kind

### 2.5.2 Hilbert Transform

## 2.6 Sobolev Spaces

Let  $L^2$  be the space of all  $2\pi$ -periodic complex functions  $f$  which are square integrable over  $[0, 2\pi]$  equipped with the inner product

$$(f, g)_2 = \frac{1}{2\pi} \operatorname{Re} \int_0^{2\pi} f(t)\overline{g(t)} dt.$$

### Definition 9

The **Sobolev space**  $W$  is defined as the space of all absolutely continuous functions  $f \in L^2$  such that the derivative  $f'$  exists and is also in  $L^2$ . The inner product on  $W$  is defined as

$$(f, g)_W = (f, g)_2 + (f', g')_2.$$

This is a Hilbert space over  $\mathbb{R}$ . The subspaces of real functions are denoted  $L_{\mathbb{R}}^2$  and  $W_{\mathbb{R}}$  respectively. Note that we can decompose  $W$  into the direct sum of the subspaces  $W = W^+ \oplus W^-$  where  $f \in L^2$  is decomposed as follows into its Fourier series:

$$f(t) = \sum_{n=-\infty}^{\infty} a_n e^{int} = \underbrace{\sum_{n=-\infty}^0 a_n e^{int}}_{=: f^- \in W^-} + i(\text{Im}(a_1))e^{int} + (\text{Re}(a_1))e^{int} + \underbrace{\sum_{n=2}^{\infty} a_n e^{int}}_{=: f^+ \in W^+}.$$

Recall the definition of  $\Phi$  as the mapping from the boundary of the disk **VIA ETA** and subject to 1. This can now be expressed as  $\Phi \in W^+$ **HUH**. Then, since the boundary function 2 maps the unit circle to  $\Gamma$  there exists **why** a function  $\hat{u}$  such that

$$\Phi(t) = \eta(t + \hat{u}(t)) \quad \forall t.$$

By the implicit function theorem 2.8  $\hat{u}$  is continuously differentiable, hence  $\hat{u} \in W_{\mathbb{R}}$ . This tells us that the function  $\Phi$  we are looking for lies in the intersection of a certain manifold  $M := \{u \in W_{\mathbb{R}} : \eta(t + u(t))\}$  with our space  $W^+$ . This formulation is used in chapter 3.3.1.

## 2.7 Riemann-Hilbert Problems

XXXXXXXXXXXXXX

## 2.8 Complex Analysis/ Function Theoretic Tools

### Definition 10

A **Möbius transform** is a function on the extended complex plane  $\hat{\mathbb{C}} := \mathbb{C} \cup \{\infty\}$  which is uniquely determined by where it sends three points. It has the form

$$f(z) = \frac{az + b}{cz + d}$$

with complex numbers  $a, b, c, d$  such that  $ad - bc \neq 0$ .

More explicitly, given three distinct points  $z_1, z_2, z_3 \in \mathbb{C}$  and three distinct points  $w_1, w_2, w_3 \in \mathbb{C}$  there exists a unique Möbius transform  $f$  such that  $f(z_i) = w_i$  for  $i = 1, 2, 3$ :

$$f(z) = \frac{(z - z_1)(z_2 - z_3)}{(z - z_3)(z_2 - z_1)}$$

In particular, Möbius transforms are conformal and more general than affine maps, since they can e.g. map  $\infty$  to 0 and vice versa.

## 2.9 Meshes

In order to numerically solve boundary value problems the domain is usually discretized by creating a mesh  $\mathcal{M}$  of  $N$  nodes (points) and  $M$  elements (cells) covering the domain  $\Omega$ .

## 2.10 Mesh Structure

In order to keep the approximation error as low as possible while maintaining good solver performance, we typically want uniform meshes, e.g. where the triangulation is close to equilateral. The quality of a mesh is measured in terms of its individual cells where for a mesh  $\mathcal{M} := \{K\}$  of triangles  $K$  such that

$$\bar{\Omega} = \cup_{K \in \mathcal{M}} K$$

we define  $d(K)$  the diameter of the smallest  $K$ -circumscribing ball (aka diameter of  $K$ ) and  $\mu(K)$  the diameter of the largest ball inscribed in  $K$ . Then a measure [Wec19] for the quality of  $K$  is the ratio of these diameters

$$\rho(K) := \frac{d(K)}{\mu(K)} \in [1, \infty).$$

## 2.11 Crowding

[Ban08] Crowding is the phenomenon that occurs when a set of more or less equally distributed points on the domain are mapped to a much more dense set of points on the target region, thereby causing numerical issues due to the angles on the grid becoming very small. This typically occurs when the target region is elongated, i.e. has a high aspect ratio. Wegmann [Weg05] proved the following result.

### Theorem 2.11

When the region  $G$  can be enclosed in a rectangle with sides  $a$  and  $b$ ,  $b \leq a$ , such that  $G$  touches both small sides then the conformal mapping  $\phi : D \rightarrow G$  satisfies

$$\|\phi'\|_D \geq b\psi(b/a)$$

with a function  $\psi(\tau)$  which behaves for small  $\tau$  like

$$\psi(\tau) \approx \frac{1}{2\pi\sqrt{\epsilon}} \exp\left(\frac{\pi}{2\tau}\right).$$

DeLillo has shown how crowding affects the accuracy of numerical computations.

### 2.11.1 The operator $R$

In some conformal mapping methods, boundary value problems as follows occur,

$$\psi(e^{it}) = B(t) + A(t)U(t)$$

where  $A, B : \mathbb{C} \rightarrow \mathbb{C}$  and  $U : \mathbb{C} \rightarrow \mathbb{R}$ . Multiplication with  $\bar{A}$  yields the RH problem

$$\operatorname{Im}(A(\bar{t})\psi(e^{it})) = \operatorname{Im}(\bar{A}(\bar{t})B(t))$$

This problem can be solved by the operator  $R_\beta$ , which is defined as follows:  
This follows from the following theorem:

**Theorem 2.12**

There exists a function  $\psi$  analytic in  $D$  with  $\psi(0) = 0$  satisfying the boundary problem if and only if  $U$  is a solution of the Fredholm integral equation of the second kind

$$(I + R_\beta)U = g$$

with the right-hand side

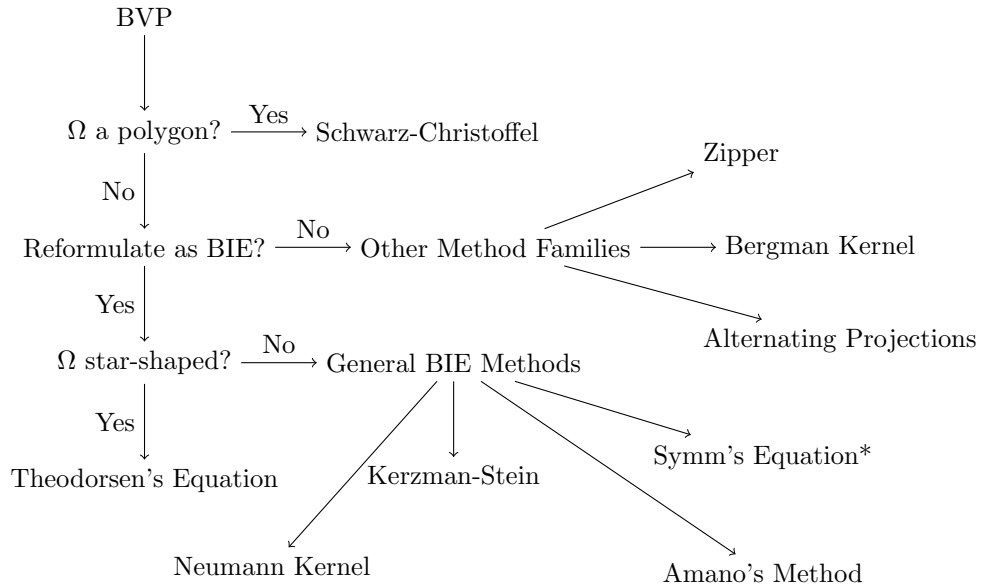
$$g := -Re(e^{-i\beta}(I - iK + J)/B).$$

Where  $K$  is the conjugation operator and  $J$  the averaging operator.

### 3 Existing Methods

This chapter aims to give an overview and compare existing methods in terms of input/output format, suitability/ boundary requirements, computational complexity, numerical stability and mesh quality preservation/ accuracy.

We give an overview of some existing methods and how to choose each depending on the application before explaining each of them in more detail.



*\*(Linear Fredholm 1<sup>st</sup> kind, generally ill-posed -*i.e.* not preferred)*

#### 3.1 Bergman Kernel Method

#### 3.2 Preprocessing

##### 3.2.1 Osculation Methods

#### 3.3 Alternating Projections Method

Various methods for numerical construction of  $\psi$  essentially construct two sequences of functions, one of normalized analytic functions on the disk (using the operator  $K$  2.3) and one mapping the boundary of  $\mathbb{D}$  to the boundary  $\Gamma$ . The method of alternating projections uses both these sequences and alternates between them to find  $\psi$  [Weg89].

**MOVE THIS TO THE BEGINNING OF THE ARTICLE** For this method we suppose  $\Gamma = \partial\Omega$  is a smooth Jordan curve parametrized by a  $2\pi$ -periodic function  $\eta(s)$  with continuous non-vanishing derivative  $\eta'(s) \neq 0$  having winding number 1 on  $[0, 2\pi]$ , i.e.  $\Gamma$  surrounds  $\Omega$  exactly once.

### 3.3.1 Alternating Projections à la von Neumann

For two closed convex sets  $P, Q$  in a Hilbert space  $H$ , the method of alternating projections constructs a sequence  $(x_n)_n$  as follows: Starting from an arbitrary point  $x_0 \in H$ , we define

$$x_{n+1} := \begin{cases} \Pi_P(x_n) & n \equiv 0 \pmod{2} \\ \Pi_Q(x_n) & n \equiv 1 \pmod{2} \end{cases}$$

where  $\Pi_P(z) = \min_{x \in P} \|x - z\|^2$  and  $\Pi_Q(z) = \min_{x \in Q} \|x - z\|^2$  denote the orthogonal projections onto the sets  $P$  and  $Q$  respectively. It can be shown that the sequence  $(x_n)_n$  converges in norm to a point tuple  $(x^*, y^*)$  satisfying

$$\begin{cases} x^* = \Pi_P(y^*), \\ y^* = \Pi_Q(x^*), \\ d_H(x^*, y^*) = \min_{(x,y) \in P \times Q} \|x - y\|^2 \end{cases}$$

In particular,  $x^* = y^*$  if  $P \cap Q \neq \emptyset$ . [BPW23]

This exact idea is now applied to function spaces:

### 3.3.2 Algorithm

---

#### Algorithm 1 AP-Method

---

Start with a function  $U_0 \in W_{\mathbb{R}}$ .

Given  $U_k$  for  $k \geq 0$ ,

**for**  $n = 1, 0, -1, -2, \dots$  **do**

$a_n = \frac{1}{2\pi} \int_0^{2\pi} \eta(t + U_k(t)) e^{-int} dt$  [Calculate Fourier coefficients]

**end for**

$U_{k+1}(t) := U_k(t) - \operatorname{Re} \frac{i(\operatorname{Im}(a_1)) e^{it} + \sum_{n=-\infty}^0 a_n e^{int}}{\dot{\eta}(t + U_k(t))}$  [Calculate the new iterate]

---

## 3.4 Schwarz-Christoffel Method

One class of methods for finding the conformal mapping  $\Phi$  is given by the Schwarz-Christoffel equation, which relates the derivative of  $\Phi$  to an integral over the boundary of the target domain  $\Omega$  when  $\Omega$  is a polygon.

### 3.4.1 Preliminaries and Notation

#### Definition 11

A **Polygon** is a planar figure whose boundary is made of a chain of connected line segments which we will call arcs, connecting corner points.

The unit disk  $\mathbb{D}$  is in particular a polygon, and we parametrize the boundaries  $\partial\mathbb{D}$  and  $\partial\Omega = \Gamma$  by collections of arcs  $s_{\mathbb{D}}$  and  $s_{\Omega}$  respectively, in positive

mathematical orientation. These arcs being smooth yields tangents with well-defined derivatives at every point of the boundary curves except for corners, and we denote the angles of these tangents with  $\theta_{\mathbb{D}}(s_{\mathbb{D}})$  and  $\theta_{\Omega}(s_{\Omega})$  respectively. If  $z_0$  is a corner it will have a turning angle of

$$\angle\theta_{\mathbb{D}}(z_0) = \theta_{\mathbb{D}}(z_0 + \varepsilon) - \theta_{\mathbb{D}}(z_0 - \varepsilon),$$

where  $\varepsilon \rightarrow 0$ . The same applies to corners of  $\Omega$ . Then,  $\frac{\partial\theta_{\mathbb{D}}}{\partial s_{\mathbb{D}}} = \angle\theta_{\mathbb{D}}(z_0)\delta(s_{\mathbb{D}} - z_0)$  for  $\delta$  the Dirac function, and similarly for  $\theta_{\Omega}$  and thus  $\theta_{\mathbb{D}}$  and  $\theta_{\Omega}$  are piecewise continuously differentiable functions with jump discontinuities at the corner points.

### 3.4.2 the log derivative of Phi

### 3.4.3 Green's Functions

A Green's function is a general concept for solving differential equations containing a linear operator.

#### Definition 12

A **Green's function** or **Green function**  $G(x, s)$  is any solution to

$$LG(x, s) = \delta(x - s)$$

where  $L = L(x)$  is a linear operator acting on distributions over  $\mathbb{R}^n$  and  $\delta$  is the Dirac delta function.

This definition can be exploited to solve inhomogeneous differential equations of the form  $Lu = f(x)$ . In the case of the SCE the Green's function are defined as  $G(z, z') : \mathbb{D} \rightarrow \mathbb{R}$  satisfying

$$\nabla^2 G(z, z') = 2\pi\delta(u - u')\delta(v - v')$$

inside the disk and

$$\frac{\partial G(z_B, z')}{\partial n} = \beta_i$$

where  $n$  is the outward normal vector at the boundary point  $z_B \in \partial\mathbb{D}$  and  $\beta_i$  is a real constant associated with the  $i$ 'th arc's length  $l_i$  such that  $\sum l_i \beta_i = 2\pi$ . It can be shown according to Floryan and Zemach that this defines a unique Green's function up to an additive constant [FZ87]. The SCE can be written explicitly whenever the Green's function is **obtainable in closed analytic form**, i.e. **expressable via a finite number of elementary operations** (is that what is meant on p348? i looked up wikipedia for closed analytic form).

### 3.4.4 Schwarz-Christoffel Equation Variants

Let  $\mathcal{G}(z, z'_B)$  be a complex extension of the above defined  $G(z, z'_B)$ , i.e.  $\mathcal{G}(z, z'_B)$  is analytic with real part  $G(z, z'_B)$ . A Schwarz-Christoffel equation for a confor-

mal mapping  $\Phi(z) : \mathbb{D} \rightarrow \Omega$  has the form

$$\log \frac{d\Phi}{dz} = C + \sum_i Q_i,$$

where  $C \in \mathbb{C}$  is a constant and the  $Q_i$  are the Green's function integrals over the boundary arcs of  $\mathbb{D}$ . Some parameters and constants have to be determined in order to get a unique  $\Phi$  for a particular given  $\Omega$ . The Riemann mapping theorem allows HOW? for the first three real parameters to be preassigned, for example to three boundary points in the case of simply connected bounded  $\Omega$ . The remaining degrees of freedom must be solved for using properties of the arcs  $s_\Omega(s_z)$  and  $s_{\mathbb{D}}(s_z)$ .

The most general form is called Schwarz-Christoffel equation with subtraction [FZ87]:

$$\log\left(\frac{d\Phi}{dz}\right) = C_0 - \frac{1}{2\pi} \int_{\partial\mathbb{D}} [\mathcal{G}(z, z'_B) - \mathcal{G}(z_0, z'_B)] \times [d\theta_\Omega(s'_z) - d\theta_{\partial\mathbb{D}}(s'_z)]$$

where  $C_0 \in \mathbb{C}$  is a constant,  $z_0$  is a fixed point in  $\mathbb{D}$  or del?,  $\mathcal{G}(z, z'_B)$  is the fundamental solution of the Laplace equation in  $\partial\mathbb{D}$  with singularity at  $z'_B \in \partial\mathbb{D}$  not at the boundary of omega?. However, we can use an unsubtracted form of this equation since the integrals converge separately and we know our  $\Omega$  is bounded (hence we need not care about behaviours at infinity), yielding the simpler form

$$\log\left(\frac{d\Phi}{dz}\right) = C - \frac{1}{2\pi} \int_{\partial\mathbb{D}} \mathcal{G}(z, z'_B) [d\theta_\Omega(s'_z) - d\theta_{\partial\mathbb{D}}(s'_z)]$$

### 3.4.5 Implementation

[Bro90] [Tre80] [BT03] [Bez22] Crowding is a problem because it yields exponential derivative of  $\Phi$ , but can be fixed. [Ban08]

## 3.5 Zipper Method

This algorithm was founded independently by Kühnau and Marshall in the 1980's has the advantage of finding  $\Phi$  and its inverse at the same time. The computed map is only approximately conformal, and is obtained as a composition of conformal maps onto slit halfplanes. Depending on the shape of the slits, the Zipper algorithm looks a bit different. In this section we will focus on the easiest version called the "geodesic algorithm" [MR06] which is quite beautiful from a geometric perspective.

### 3.5.1 The Geodesic Algorithm

The most elementary version of this algorithm is based on a function

$$f_a : \mathbb{H} \setminus \gamma \rightarrow \mathbb{H}$$

where  $\mathbb{H}$  is the upper half plane and  $\gamma$  is a circular arc from 0 to  $a \in \mathbb{H}$  which is orthogonal to the real axis. The orthogonal circle also meets the real axis again at  $b = |a^2|/Im(a)$ . Then the map can be expressed in closed form as

$$f_a(z) = \sqrt{g_a \circ h_a(z)}$$

where  $g_a(z) = z^2 + c^2$  and  $h_a(z) = \frac{z}{1-z/b}$ .

**INSERT IMAGE**

Now suppose  $z_0, z_1, \dots, z_n$  are points arranged counterclockwise on a Jordan curve  $\Gamma$  in the upper half plane. The geodesic algorithm basically iterates over the arcs from  $z_i$  to  $z_{i+1}$  and "unzips" them one by one using the map  $f_{a_i}$  where  $a_i$  is the image of  $z_{i+1}$  under the composition of all previous maps. The original geodesic algorithm proposed by Marshall and Rohde constructs a conformal map from the upper half plane to the region bounded by  $\Gamma$ , but it can be adapted to map from the unit disk as well via a Möbius transformation mapping the half plane to the unit disk and back first (hopefully?).

---

### Algorithm 2 Geodesic Zipper Algorithm

---

**Input:** Points  $z_0, z_1, \dots, z_n$  on a Jordan curve  $\Gamma$  in the upper half plane.  
**Output:**  $\psi$ : conformal map from  $\mathbb{H}$  to the region bounded by  $\Gamma$  and its inverse  $\psi^{-1}$ .

```

 $\phi_1(z) := i\sqrt{(z - z_1)/(z - z_0)}$ 
 $\zeta_2 := \phi_1(z_2)$ 
 $\phi_2(z) := f_{\zeta_2}(z)$ 
for k in n do
     $\zeta_k := \phi_{k-1} \circ \dots \circ \phi_1(z_k)$ 
     $\phi_k(z) := f_{\zeta_k}(z)$ 
end for
Finally,  $\zeta_{n+1} := \phi_n \circ \dots \circ \phi_1(z_0) \in \mathbb{R}$  and  $\phi_{n+1}(z) := -(\frac{z}{1-z/\zeta_{n+1}})^2$ 
Then  $\psi(z) := \phi_1^{-1} \circ \phi_2^{-1} \circ \dots \circ \phi_{n+1}^{-1}(z)$  and  $\psi^{-1}(z) := \phi_{n+1} \circ \dots \circ \phi_2 \circ \phi_1(z)$ 
```

---

**INSERT IMAGE**

### 3.5.2 The Slit Algorithm

The above geodesic algorithm is only as accurate as the approximation of the boundary curve  $\Gamma$  by circular arcs between the points  $z_i$ . A more accurate version is given by the slit algorithm, which uses straight line segments instead of circular arcs. We therefore exchange the map  $f_a$  for a map  $g_a : \mathbb{H} \setminus L \rightarrow \mathbb{H}$  where  $L$  is the line segment from 0 to  $a \in \mathbb{H}$ . This map does not have a closed form expression, but can be computed numerically using Newton's method.

### 3.5.3 The Zipper Algorithm

The approximation of  $\Gamma$  by circular arcs or straight line segments can be further improved by using circular arcs which meet  $\Gamma$  tangentially at the points  $z_i$ .

Each arc is determined by the points  $z_i, z_{i+1}$  and  $z_{i+2}$ , hence we assume an even number of boundary points. The first arc is replaced by

$$\phi_1(z) = \sqrt{\frac{(z - z_2)(z_1 - z_2)}{(z - z_0)(z_1 - z_2)}}.$$

At each subsequent step that circular arc through  $\zeta_k$  and  $\zeta_{k+1}$  is mapped onto a straight line segment by a Möbius transform, and then the Slit Algorithm is applied to unzip that segment. This yields a sort of "quadratic approximation" of  $\partial\Omega$  instead of a linear one.

GOOD PAPER FOR IMPLEMENTATION ESPECIALLY END NOTES

### 3.6 Newton/ Wegmann Method

For smooth  $\partial\Omega$ , Integral equations of the second kind can also be solved by Newton's method [Weg78]. Let  $\eta$  be a differentiable parametrization of  $\Gamma$  and  $\dot{\eta}(s) \neq 0 \forall s$ .

Let  $S(\zeta)$  be a  $2\pi$ -periodic function such that  $\psi(\zeta) = \eta(S(\zeta))$ .

$$\begin{array}{ccccc} \mathbb{D} & \xrightarrow{S} & [0, 2\pi] & \xrightarrow{\eta} & \Gamma \\ & \curvearrowright & & & \end{array}$$

$\psi$

We approximate the conformal map  $\psi$  as follows: Assume that the approximation for  $\psi$  after  $k$  steps be given by  $\psi_k(\zeta) = \eta(S_k(\zeta))$ . We improve the approximation by moving the points along the tangent towards the boundary curve, i.e. by finding a correction function  $U_k : \partial\mathbb{D} \rightarrow [0, 2\pi]$  such that

$$\eta(S_k(\zeta)) + U_k(\zeta)\dot{\eta}(S_k(\zeta)) = h_{k+1}(\zeta) \quad (4)$$

where  $h$  is analytic on  $\overline{\Omega}$  and  $h_{k+1}(\zeta)$  is the boundary value of the next approximation  $\psi_{k+1}(z_n) = c_n$ . For the boundary point  $z_0$  we are given  $c_0 = \eta(s_0) \in \Gamma$ . Note that since  $h_{k+1}(z_0)$  lies on the tangent through  $\eta(S_k(z_0))$  we cannot have  $h_{k+1}(z_0) = c_0$  unless  $\eta(S_k(z_0)) = c_0$ . Therefore we set

$$U_k(z_0) = s_0 - S_k(z_0). \quad (5)$$

Note also that  $h_{k+1}$  is an approximation of  $\psi$  but it does not generally take values on  $\Gamma$ . We get an approximation for the parametrization  $S$  by

$$S_{k+1}(\zeta) := S_k(\zeta) + U_k(\zeta).$$

#### 3.6.1 Implementation

Since we assume  $\psi$  to map from the unit disk  $\mathbb{D}$ , the integral equations can be explicitly solved by discretization and trigonometric interpolation: Take  $N = 2n$  equidistant points  $\zeta_k = e^{i\theta_k}$  on the boundary of the disk, where

$$\theta_k = \theta_0 + \frac{\pi k}{n}, \quad k \in [2n - 1]$$

and write the integrals in terms of their Fourier transform

$$F(z) = \frac{1}{2\pi i} \int \frac{\sigma_n(\zeta)}{\zeta - z} d\zeta \quad (6)$$

where  $\sigma_n(\zeta_k) = \sum_{i=-n}^n c_k \zeta_k^i$ . This can be computed fast ( $\in \mathcal{O}(n \log n)$ ) via FFT. Each iteration is computed via interpolating polynomials.

### 3.7 Theodorsen's Method

probably put this before wegmann method

We can reformulate the problem of finding the conformal mapping  $\psi : \mathbb{D} \rightarrow \Omega$  as solving Theodorsen's integral equation for the boundary correspondence function  $\theta(s)$  rename theta to S? defined by

$$\psi(e^{is}) = \eta(\theta(s)) \text{ and } \int_0^{2\pi} \theta(s) ds = 2\pi^2 \quad (7)$$

where  $\eta$  is a parametrization of  $\Gamma = \partial\Omega$ .  $\psi$  is assumed to be normalized such that  $\psi(0) = 0$  and  $\psi'(0) > 0$ . Theodorsen's integral equation states that  $Y : s \mapsto \theta(s) - s$  is the conjugate periodic function of  $X : s \mapsto \log(\eta(\theta(s)))$ . After discretization, Theodorsen's integral equation becomes the fixed point equation

$$y = \Psi(y) := K_\Sigma \log(\eta(s + y)) \quad (8)$$

for  $s := (\frac{k\pi}{N})_{k \in [2N-1]}$  where  $y$  approximates  $Y(s)$ . The product  $y$  can be computed efficiently using FFT (see 2.3). If the discretization is based on trigonometric interpolation,  $K_\Sigma$  is called **Wittich's matrix** [Gut83]. By a permutation  $P$  the above components can be brought to the form

$$PK_\Sigma P = \begin{pmatrix} 0 & -L^T \\ L & 0 \end{pmatrix}, \quad Py = \begin{pmatrix} y'' \\ y' \end{pmatrix}, \quad Ps = \begin{pmatrix} s'' \\ s' \end{pmatrix}. \quad (9)$$

By Niethammer, (8) can be solved using nonlinear successive over-relaxation (SOR) for given  $y_0$ ,  $y'_0$  and  $\omega$  (relaxation factor) and  $m \geq 0$ :

$$\begin{aligned} y''_{m+1} &:= (1 - \omega) y''_m - \omega L^T \log(\eta(s' + y'_m)) \\ y_{m+1} &:= (1 - \omega) y'_m + \omega L \log(\eta(s'' + y''_m)) \end{aligned} \quad (10)$$

Alternatively, nonlinear Jacobi iteration with relaxation (JOR) can be used:

$$y_{m+1} := (1 - \omega) y_m + \omega \Psi(y_m). \quad (11)$$

In case of  $\Gamma$  not being smooth, Theodorsen's method becomes inaccurate [Gut83]. In this case, the boundary curve can be smoothed first using preliminary maps see osculation methods.

Theodorsen's method 3.7 needs  $\Omega$  to be star-shaped in order to converge [Weg78] and is particularly simple (fixed point equation) in this case. In practice, the star-shape requirement can be relaxed by smoothing the boundary curve first using preliminary maps [Gut83].

### 3.8 Conjugate Function Method

Hakula, Quach and Rasila [HQR13] presented a new method in 2010 which is based on numerical solution of the Laplace equation subject to Dirichlet-Neumann mixed-type boundary conditions by using *hp*-FEM. In their paper they construct the mapping starting from a quadrilateral, but it can be tweaked to map from the unit disk as well. "It is well known that one can express the modulus of a quadrilateral  $Q$  in terms of the solution of the Dirichlet-Neumann mixed boundary value problem [FIND HENRICI'S BOOK, p. 431]."

### 3.9 Amano's Method of Fundamental Solutions

[Sak19] jordan region [Ama98]

### 3.10 Probabilistic Uniformization Method

In 2007, Binder, Braverman and Yampolsky proposed a method for finding a conformal map using a random walks solver to the general Dirichlet problem. They conjectured an upper bound of polynomial space and time for an algorithm with precision  $\frac{1}{n}$  pixels (for explicitly given  $\partial\Omega$ ; quadratic if  $\partial\Omega$  is given only approximately, via a so-called *oracle*, sort of a Dirac delta function). [BBY07]

### 3.11 Comparison

The accuracy of the conformal mapping depends to a large extent on the smoothness of the boundary curve  $\Gamma$ . Wegmann [Weg05] section 2.5 proved that accuracy of methods based on function conjugation is bounded by the error of the operator  $K_N$  of the conjugation operator on the grid 2.3. Theodorsen's method is known [Gai64] add page/argument to have an error of order  $O(R^{-n})$  for regions bounded by analytic curves, where  $R > 1$  is the index of the largest disk centered at the origin to which the boundary parametrization  $\eta$  can be extended as a conformal map, and  $n$  is the order of the polynomials approximating  $\eta$ . Wegmann compared the accuracies of the AP, OAP, Theodorsen and Wegmann methods for the mapping from the disk to an inverted ellipse example 4? and found that OAP is most efficient for low accuracy and Newton methods are best for high accuracy calculations [Weg05] p.415.add figure? Note the computational costs are mainly determined by the FFTs and this parameter is dependent on the number of grid points.

The AP Method converges linearly if the boundary parametrization is 3-Hölder and the initial approximation  $U_0$  is sufficiently close to the actual boundary correspondence function  $\eta(s)$  [Weg89] p.292. Fourier calculation can be done very efficiently using FFT which makes AP one of the simplest and most robust methods for conformal mapping. However, it is also not very accurate for reasonably sized grids, and converges very slowly for finer meshes [Weg05] p. 389.

GMRES or CGS or SOR(Niethammer) for solving linear IER (Amano, Kerzman-Stein)

The Newton method converges locally quadratically if the domain is the unit disk  $\mathbb{D}$ . Generally, the algorithm can achieve space efficiency of  $\mathcal{O}(n)$  and computational efficiency of  $\mathcal{O}(n^2)$  or  $\mathcal{O}(n \log n)$  if FFT is used, just like in the conjugate function method. [Weg78] [Weg84]

Marshall and Rohde [MR06] proved that if  $\Gamma = \partial\Omega$  is a  $C^{3/2}$  closed Jordan curve with points  $\{z_i\} \subset \partial\Omega$  having mesh size  $\mu = \max|z_j - z_{j+1}|$  there is a constant  $C$  depending on the geometry of  $\partial\Omega$  such that the conformal map  $\psi$  found by the zipper algorithm satisfies accuracy of  $\mathcal{O}(C\mu^{3/2})$ . The geodesic algorithm works only with elementary functions, as a result its speed depends only on the number of points on the boundary (i.e. mesh size) and not on the shape of the region. The accuracy can be measured explicitly if the true conformal map is known, which is our case. **ADD COMPUTATION AND IMAGES LIKE IN MnR'S PAPER i3**

The FFT is used in any method that needs to repeatedly calculate the conjugate function (the Hilbert transform) on a regular grid on the unit circle. enhances runtime from  $n^2$  to  $n \log n$

Table 1: Overview Table

Algorithm	$\Omega$ shape	Runtime	Space	Input	Output	Advantages	Disadvantages
Alternating projections	shape	Runtime	Space	Input	Output	Advantages	Disadvantages
Zipper	shape	Runtime	Space	Input	Output	Advantages	Disadvantages
Theodorsen	star-shaped	Runtime	Space	Input	Output	Advantages	Disadvantages
Schwarz-Christoffel	polygon	Runtime	Space	Input	Output	corner-handling	disadvantages
Nietzhammer	shape	Runtime	Space	linear system of equations	Output	Advantages	Disadvantages
Wegmann	shape	Runtime	Space	non-linear Theodorsen Equation	Output	Advantages	Disadvantages
Conjugate fct	shape	Runtime	Space	Input	Output	Advantages	Disadvantages
Spare row	shape	Runtime	Space	Input	Output	Advantages	Disadvantages

## 4 Proposed Method

### 4.1 Choice/ Justification

criteria: - Accuracy for domains with sharp corners or high curvature - Speed for practical mesh sizes - Robustness - does it fail for certain domain shapes? - Implementation complexity given your timeline - Jacobian computation - analytical vs numerical differentiation

### 4.2 Implementation

- Separate modules for boundary parameterization, mapping computation, Jacobian eval, and mesh transformation - plot original vs. mapped grids (e.g., Matplotlib quiver for Jacobians) to spot issues early.

### 4.3 Numerical Experiments/ Testing

check angle preservation (e.g., via dot products on mapped vectors) and scale factors ( $\det(D\Phi) > 0$ ,  $|\frac{\partial \Phi}{\partial z}|$  constant in theory). - Test suite: Use known exact mappings (e.g., disk to square via Schwarz-Christoffel) for error metrics (L2 norm on boundary points). - Metrics: Runtime for N points, mesh quality post-mapping (e.g., min/max angles in triangles, shape regularity ratio). - Real-world applicability: Apply to a sample FEM problem (e.g., Poisson equation on  $\Omega$ ) and compare accuracy/speed vs. uniform mesh. - Robustness: Vary boundary complexity (smooth vs. corners), noise in Fourier coeffs, mesh resolutions. - Debugging: Use assertions for bijectivity (e.g., check injectivity numerically) - Error handling - what happens with degenerate inputs?

### 4.4 Results

## **5 Conclusion**

## **6 Documentation and Implementation**

### **6.1 Testing (again?)**

**VALIDATION AGAINST THE SCHWARZ-CHRISTOFFEL TOOLBOX!**

## References

- [Ama98] Kaname Amano. A charge simulation method for numerical conformal mapping onto circular and radial slit domains. *SIAM Journal on Scientific Computing*, 19(4):1169–1187, 1998.
- [Ban08] L. Banjai. Revisiting the crowding phenomenon in schwarz–christoffel mapping. *SIAM Journal on Scientific Computing*, 30(2):618–636, 2008.
- [BBY07] Ilia Binder, Mark Braverman, and Michael Yampolsky. On computational complexity of riemann mapping, 2007.
- [Bez22] S. I. Bezrodnykh. Lauricella function and the conformal mapping of polygons. *Mathematical Notes*, 112(4):505–522, 2022.
- [BPW23] Gábor Braun, Sebastian Pokutta, and Robert Weismantel. Alternating linear minimization: Revisiting von neumann’s alternating projections, 2023.
- [Bro90] Philip Raymond Brown. *The use of the Schwarz-Christoffel transformation in finite element mesh generation*. Phd, University of Leices- ter, 1990.
- [BT03] Lehel Banjai and L. N. Trefethen. A multipole method for schwarz–christoffel mapping of polygons with thousands of sides. *SIAM Journal on Scientific Computing*, 25(3):1042–1065, 2003.
- [CR25] René E. Castillo and Edixon M. Rojas. Revisiting the hilbert transform of periodic functions. *Mathematische Semesterberichte*, 72:29–49, 2025.
- [EW22] Manfred Einsiedler and Andreas Wieser. Analysis i und ii. Vorlesungsskript 2021/2022, 2022.
- [FZ87] J.M Floryan and Charles Zemach. Schwarz-christoffel mappings: A general approach. *Journal of Computational Physics*, 72(2):347–371, 1987.
- [Gai64] Dieter Gaier. *Konstruktive Methoden der konformen Abbildung*, volume 3 of *Springer Tracts in Natural Philosophy / Ergebnisse der ange- wandten Mathematik*. Springer-Verlag, Berlin, Göttingen, Heidelberg, 1964.
- [Gut83] Martin H. Gutknecht. Numerical experiments on solving theodorsen’s integral equation for conformal maps with the fast fourier transform and various nonlinear iterative methods. *SIAM Journal on Scientific and Statistical Computing*, 4(1):1–30, 1983.

- [HQR13] Harri Hakula, Tri Quach, and Antti Rasila. Conjugate function method for numerical conformal mappings. *Journal of Computational and Applied Mathematics*, 237(1):340–353, January 2013.
- [MR06] Donald E. Marshall and Steffen Rohde. Convergence of the zipper algorithm for conformal mapping, 2006.
- [Pom92] Christian Pommerenke. *Boundary Behaviour of Conformal Maps*, volume 299 of *Grundlehren der mathematischen Wissenschaften*. Springer-Verlag, Berlin, 1992.
- [Sak19] Koya Sakakibara. Bidirectional numerical conformal mapping based on the dipole simulation method, 2019.
- [SS03] Elias M. Stein and Rami. Shakarchi. *Complex analysis*. Princeton lectures in analysis ; 2. Princeton University Press, Princeton, N.J, 2003.
- [Tre80] Lloyd N. Trefethen. Numerical computation of the schwarz–christoffel transformation. *SIAM Journal on Scientific and Statistical Computing*, 1(1):82–102, 1980.
- [Wec19] F Wechsung. *Shape optimisation and robust solvers for incompressible flow*. PhD thesis, University of Oxford, 2019.
- [Weg78] Rudolf Wegmann. Ein iterationsverfahren zur konformen abbildung. *Numerische Mathematik*, 30(4):453–466, 1978.
- [Weg84] Rudolf Wegmann. Convergence proofs and error estimates for an iterative method for conformal mapping. *Numerische Mathematik*, 44:435–461, 1984.
- [Weg89] Rudolf Wegmann. Conformal mapping by the method of alternating projections. *Numerische Mathematik*, 56:291–307, 1989.
- [Weg05] Rudolf Wegmann. Chapter 9 - methods for numerical conformal mapping. In R. Kühnau, editor, *Geometric Function Theory*, volume 2 of *Handbook of Complex Analysis*, pages 351–477. North-Holland, 2005.